


Article

# Molecular Cloning and Structure–Function Analysis of a Trypsin Inhibitor from Tartary Buckwheat and Its Application in Combating Phytopathogenic Fungi

Jing-jun Ruan <sup>1</sup> , Shan-jun Tian <sup>1</sup>, Jun Yan <sup>2,3</sup>, Hui Chen <sup>4</sup>, Ru-hong Xu <sup>1</sup>  
and Jian-ping Cheng <sup>1,\*</sup>

<sup>1</sup> College of Agriculture, Guizhou University, Guiyang 550025, China;

chenggy508@sohu.com (J.-j.R.); jjruan@gzu.edu.cn (S.-j.T.); rhxu@gzu.edu.cn (R.-h.X.)

<sup>2</sup> Institute of Evolution, University of Haifa, Haifa 31905, Israel; jyan@cdu.edu.cn

<sup>3</sup> School of Pharmacy and Bioengineering, Chengdu University, Chengdu 610106, China

<sup>4</sup> College of Life Science, Sichuan Agriculture University, Ya'an 625014, China; hchen@sicau.edu.cn

\* Correspondence: ruanj741@aliyun.com; Tel.: +86-0851-83855894

Received: 10 January 2018; Accepted: 10 April 2018; Published: 12 April 2018



**Abstract:** Host plant protease inhibitors offer resistance to proteases from invading pathogens. Trypsin inhibitors (TIs), in particular, serve as protective agents against insect and pathogen attacks. In this study, we designed a pair of degenerate primers based on highly conserved motifs at the N- and C-termini of the TI from tartary buckwheat (*Fagopyrum tataricum*; *Ft*) to clone the central portion. Genomic walking was performed to isolate the 5' and 3' flanking regions of *FtTI*. We demonstrated the successful PCR amplification of a 644 bp portion of *FtTI*. The full-length DNA of *FtTI* contains a complete open reading frame of 264 bp, encoding 87 amino acids with a mass of approximately 9.5 kDa. The *FtTI* protein sequence was 49% identical and 67% similar to potato protease inhibitors. Site-directed mutagenesis identified the residues, Asp<sup>67</sup> and Arg<sup>68</sup>, as crucial for the inhibitory activity of the *FtTI*. Recombinant and mutant *FtTI* inhibited both the hyphal growth and spore germination of *Alternaria solani*. The calculated 50% inhibitory concentrations of *FtTI* ranged from 5–100 µg mL<sup>-1</sup> for spore germination and 1–50 µg mL<sup>-1</sup> for fungal growth. Thus, recombinant *FtTI* may function in host resistance against a variety of fungal plant pathogens.

**Keywords:** tartary buckwheat; trypsin inhibitor; genome walking; phytopathogenic fungi

## 1. Introduction

Fungal pathogens have a major influence on agricultural crop yields and are a very serious threat to global food security. Traditional measures of disease control rely heavily on chemical methods which have allowed farmers to overcome many common plant diseases [1]. Early blight of tomato caused by *Alternaria solani* is an important fungal disease worldwide. The most used and effective control method is the application of synthetic chemical fungicides. However, they are generally used in excess, causing environmental contamination and human health problems, and can even lead to the emergence of pathogen-resistant strains [2]. Therefore, alternative products, such as natural products from plant extracts, should be developed to reduce the dependence on synthetic chemical fungicides. Exposure to severe environments and evolution have allowed plants to develop efficient protective mechanisms against phytopathogens. Among these, plant proteins exhibiting toxic or antimetabolic activities toward pathogens are of great interest. The roles played by antifungal proteins in plant defense have been well studied [1]. These proteins, such as protease inhibitors, can provide an obstacle during the early stages of infection. Protease inhibitors are also considered protective

proteins because they suppress the activity of proteolytic enzymes of both pathogenic microorganisms and herbivorous pests that try to penetrate the host plant tissues [3]. There is growing interest in the use of plant protease inhibitors for the protection of agricultural crops, owing to their low toxicity to mammals and low persistence in the environment. Protease inhibitors that suppress the activity of specific proteases are present in animals, plants, and microorganisms [4,5]. The best studied are the serine protease inhibitors. These have been found in many plant species in which they participate in the defense against phytophagous insects and microorganisms. Plant protease inhibitors have been isolated and characterized from *Leguminosae*, *Solanaceae*, *Gramineae*, and *Cruciferae* [6–8]. In their defense against natural enemies, plants have formed a variety of protease inhibitors, the best-characterized being members of four different families: the Kunitz-type (18–22 kDa), the Bowman–Birk (8–10 kDa), the Kazal (6–8 kDa), and potato protease inhibitor I (10–14 kDa) [9]. In these four families, the reactive P1 residue is always an arginine or lysine [9,10]. The active sites of plant protease inhibitors result from their capacities to form stable complexes with microbial secreted proteases; these complexes then block, alter, or prevent access to the microbial proteolytic enzymes' active sites.

To clone an unknown target gene, it is often necessary to perform a multiple sequence alignment that includes the amino acid sequence of the known protein. Successful cloning usually relies on the identification of clear blocks of conserved regions in multiple global alignments [11]. Therefore, the alignment quality must be high. However, in many cases, degenerate primers designed using multiple sequence alignments are unsuccessful, owing to the poor conservation among the amino acid sequences being studied. To overcome this problem, Boyce et al. suggested a method of designing degenerate primers that can be used for sequencing without well-conserved blocks in multiple sequence alignments [12]. The technique is based on multiple sequence alignments using the consensus degenerate hybrid oligonucleotide primers (CODEHOPs) to identify conserved regions that are long enough to serve as primers [12,13]. The 3'-degenerative structure of consensus degenerate hybrid oligonucleotide primers allows a wide PCR specificity for remotely relevant goal gene templates, while the 5'-consensus clamp permits the strong amplification from PCR product templates during the later PCR amplification cycles. The CODEHOP method has been applied to characterize novel genes and distinguish unknown plant protease inhibitors. It has been particularly useful for remotely relevant targets and with a finite template in complicated mixtures. Three rounds of successive PCR amplifications by locus-specific and walker primers and their corresponding nested primers can effectively amplify flanking DNA fragments [14]. Only the correct degenerate primers are designed to ensure that a certain percentage of primers can be paired with the template correctly [15]. Simultaneous high-throughput three-step PCR-based genome walking, followed by direct sequencing of PCR-amplified fragments with specific nested sequencing primers may enable the development of new research strategies for gap closure in genome-assembly projects [16]. The rapid PCR-based DNA walking can be performed with any plant genomic DNA to walk directionally from any sequence-tagged site. It is a rapid and reliable way of randomly introducing unique walker primer-binding sites into different regions of the genome by annealing long synthetic oligonucleotides with partial degeneracy at the 3' or 5' end, for proper annealing and then extending with DNA polymerase.

Buckwheat is divided into two major species with agricultural significance, common (*Fagopyrum esculentum* Moench) and tartary (*Fagopyrum tataricum* Gaertn) buckwheat [17]. Tartary buckwheat is widely cultivated in the southwestern mountains of China and grows mainly on the Yunnan–Guizhou Plateau (altitude range: 2100–3400 m above sea level). Common buckwheat protease inhibitors have remarkable functions and anti-inflammatory, anti-leukemia, anticancer, anti-bollworm, and anti-plant fungal disease effects [18–23]. However, there are relatively few studies on tartary buckwheat protease inhibitors. In recent years, we have isolated and purified a trypsin inhibitor (TI) of tartary buckwheat (*FtTI*) in vitro [24], and have cloned and expressed the corresponding gene in *Pichia pastoris* [25]. However, we do not know the structure of the promoter sequence or if it has an intron sequence. Moreover, the expression level of *FtTI* in *P. pastoris* is relatively low; therefore, we wished to clone *FtTI* and express it in *Escherichia coli* for tomato fungal defense. The protease inhibitor active site's

amino acid residues play critical roles in their inhibitory functions, and if a mutation occurs in the site, it loses nearly 100% of its inhibitory activity. An arginine or lysine residue must be present in the P1 subsite for trypsin inhibition [10]. To reveal the molecular mechanism associated with the inhibitory effect of *FtTI* toward animal proteases and proteases present in plant-pathogenic microorganisms, the nucleotide sequences of 86 protein residues and three mutants of *FtTI* were artificially synthesized by PCR amplification and independently expressed by fusion in *E. coli* DE3. The recombinant protein was purified by one-step affinity chromatography and its activity against plant-pathogenic fungi was evaluated.

## 2. Materials and Methods

### 2.1. Experimental Materials

The Genome Walking Kit, restriction endonucleases, TaKaRa Mutant BEST Kit and T4 DNA ligase were purchased from TaKaRa (Shiga, Japan). *E. coli* DH5a obtained from Novagen was used for cloning and nucleotide sequencing. *E. coli* BL21 and vector pET-32a were obtained from Invitrogen. The T-A cloning vector pMD19-T was obtained from TaKaRa, and was used to construct recombinant plasmids for subcloning and sequencing.

### 2.2. Cloning of the *FtTI* Gene

#### 2.2.1. Nucleic Acid Preparation

DNA and RNA were isolated from tartary buckwheat using the MiniBEST Universal Genomic DNA Extraction Kit and the RNAiso plus Total RNA Extraction Kit (TaKaRa), respectively, unless otherwise stated. DNA and RNA concentration and purity were determined by measuring optical density at 260 and 280 nm using a spectrophotometer (SHIMADZU Uvmini-1240, Kyoto, Japan). RNase and DNase were added during the extraction procedure for DNA and RNA, respectively, and negative controls were run with each. First-strand cDNA was synthesized using Reverse Transcriptase M-MLV (TaKaRa) and oligo (dT) priming on DNase-treated RNA.

#### 2.2.2. cDNA Cloning of the Central Fragment of *FtTI*

Degenerate PCR primers (Table 1) were designed to amplify an internal fragment of *FtTI* based on the conserved regions of several protein sequences of known protease inhibitors obtained from the NCBI Protein Sequence Database. Multiple alignments of amino acid sequences were performed with CLUSTAL-W2 software, and highly conserved amino acid motifs were compared.

**Table 1.** Primers used in this study.

Primer Name	Primer Sequence (5'→3')	Purpose
CAAP1	TGG CCN GAR CTN GTT GGA	Conservative area DNA
CAAP2	RAC NCA YAC NCG GTC ACA	Conservative area DNA
SP1	TCA CAA CGA AAG TCG AAA GTG C	5' Genome walking
SP2	GGT GGC TAG AGT GGT TAA AGG AGG	5' Genome walking
SP3	CTT CCC TTT GGT TCC AAC AAG C	5' Genome walking
SP4	ACC CGG TCA CAA CGA AAG TC	3' Genome walking
SP5	CAC AAC GAA AGT CGA AAG GTC	3' Genome walking
SP6	GTG CGG CAG GTG GCT AGA GT	3' Genome walking
Fusion expression P1	CCG GAA TTC CAT GTT AAT TTA CGC TAA AGT T	Fusion expression of gene
Fusion expression P2	GAA TGC GGC CGC ACC GAC GGT TGG GGT	Fusion expression of gene
SMP1	CGT TGT GAC CTG GTG CGT GTT TTA A	Site mutation, R68L
SMP2	AAA GTG CGG CAG GTG GCT AGA GTG G	Site mutation, R68L
SMP3	CTT TCG TTG TGT CCG GGT GCG TGT T	Site mutation, D67V
SMP4	TCG AAA GTG CGG CAG GTG GCT AGA G	Site mutation, D67V
SMP5	CTT TCG TTG TGT CCT GGT GCG TGT T	Site mutation, D67V, R68L
SMP6	TCG AAA GTG CGG CAG GTG GCT AGA G	Site mutation, D67V, R68L

### 2.2.3. Genome Walking

The 5' and 3' flanking regions of *FtTI* were isolated with the Genome Walking Kit (TaKaRa) according to the manufacturer's instructions. Primary and nested PCRs were performed with forward primers complementary to the adaptor sequence (adaptor primers (AP) 1, 2, and 3 provided with the kit), and *FtTI* gene-specific primers (GSPs) 1, 2, and 3, corresponding to residues 20–43, 67–90, and 110–133, respectively, which were designed based on the cDNA-cloned central fragment of *FtTI*.

### 2.3. Site-Directed Mutagenesis

Site-directed mutagenesis and sequence assays were carried out as described previously [26–28]. *FtTI* genes with point mutations were independently introduced into the cloning vector pMD19-T by PCR. The forward and reverse oligonucleotide primers (Table 1) were complementary to the opposite strands of the vector and contained the desired mutations in the middle of the primers. Extensions with these primers generated mutated plasmids at the relevant sites. Each PCR had a total volume of 50  $\mu$ L, containing 5.0  $\mu$ L of 10 $\times$  Pyrobest Buffer II, 4.0  $\mu$ L of 2.5 mM dNTP mixture, 1.0  $\mu$ L of each primer (20  $\mu$ M), 0.25  $\mu$ L of Pyrobest DNA polymerase and 0.5 ng of pMD19-*FtTI* plasmid DNA. Sterilized distilled water was added to 50  $\mu$ L. The reaction scheme was as follows: one cycle of initial denaturation (95  $^{\circ}$ C for 4 min), 30 cycles of amplification with a lower annealing temperature (94  $^{\circ}$ C for 30 s, 56  $^{\circ}$ C for 45 s, and 72  $^{\circ}$ C for 5 min), and cooling to 4  $^{\circ}$ C. The PCR products were subjected to a blunting reaction, in which the PCR had a total volume of 50  $\mu$ L, containing 1 pmol DNA fragment, 2  $\mu$ L of 10 $\times$  Blunting Kination Buffer, 1  $\mu$ L Blunting Kination Enzyme Mix and up to 20  $\mu$ L ddH<sub>2</sub>O. The PCR program was as follows: 37  $^{\circ}$ C for 10 min and then 70  $^{\circ}$ C for 10 min. Approximately 0.25 mmol (5  $\mu$ L) of this solution was added to a microcentrifuge tube in which the ligation reaction was carried out. Ligation Solution I (5  $\mu$ L) was added and mixed well. The reaction solution was completely transformed into 100  $\mu$ L competent cells. The reaction was carried out for 1 h at 16  $^{\circ}$ C. All constructs were confirmed by direct DNA sequencing.

### 2.4. Expression of *FtTI* and *FtTI* Mutants in *E. coli*

No start and stop codon regions of *FtTI* and the *FtTI* mutants, which were independently inserted into the *E. coli* expression vector pET32a (Novagen), were amplified by PCR. The pET-32 series was designed for the cloning and high-level expression of peptide sequences fused with the 109 amino acid Trx-Tag<sup>TM</sup> thioredoxin protein. The expression vectors were independently introduced into *E. coli* BL21 Star (DE 3) cells, and gene expression was induced by the addition of 0.5 mM isopropyl  $\beta$ -D-1-thiogalactopyranoside when the culture reached an optical density of 0.65 at 600 nm. After induction and growth overnight at 30  $^{\circ}$ C, the cells expressing *FtTI* and its mutants were centrifuged at 4000 $\times$  g for 15 min, and 1 mL aliquots of the spent medium were placed in individual vials for further analyses.

### 2.5. Affinity Purification of *FtTI* and *FtTI* Mutants

His-tagged *FtTI* and *FtTI* mutants were individually affinity-purified by nickel-agarose chromatography using a protocol described previously [9]. After elution from the nickel-agarose column, the proteins were dialyzed against 50 mM phosphate buffer pH 6.8, 500 mM NaCl, 1 M (NH<sub>4</sub>)<sub>2</sub>SO<sub>4</sub>, 2 mM dithiothreitol. To evaluate purity, dialyzed fractions of purified protein were subjected to SDS-PAGE followed by Coomassie Brilliant Blue staining [22].

### 2.6. Molecular Weight Determination and Western Blot Analysis

The purified recombinant protein was subjected to SDS-PAGE using a 12.5% and 4% polyacrylamide slab gel system as described by Laemmli [29], and then transferred to a polyvinylidene fluoride membrane (Millipore, Burlington, MA, USA) using 100 mM *N*-cyclohexyl-3-aminopropanesulfonic acid buffer, pH 11, at 100 V for 30 min [30]. After blocking with skim milk, the membrane was rinsed twice

for 5 min with 25 mL Tris buffered saline–Tween (TBS–T). The blot was placed in a box containing 3 mL mouse anti-histidine for 1 h. The membrane was rinsed three times for 5 min in TBS–T and then moved to a sealed box with 3 mL goat anti-mouse alkaline phosphatase-conjugated IgG for 1 h. After incubation, the membrane was rinsed four times with 25 mL TBS–T. Then, the membrane was soaked in 25 mL alkaline phosphatase buffer for 2 min. After washing away the buffer, 5 mL color substrate solution with 50  $\mu$ L 5-bromo-4-chloro-3-indolyl phosphate and 50  $\mu$ L tetranitroblue tetrazolium chloride was applied. The color reaction was allowed to proceed in the dark for approximately 20 min.

### 2.7. Determination of Recombinant FtTI Inhibitory Activity

Trypsin inhibitory activity on bovine pancreatic and tomato early blight trypsins were determined by the method of [8]. Different concentrations of TI were incubated with  $5.6 \times 10^{-7}$  M trypsin (final concentration in 1.5 mL assay volume) for 15 min at 30 °C in 67 mM K/Na-phosphate buffer, pH 6.8. After 15 min incubation, 1.0 mL of 0.5 mM *N*-benzoyl-DL-arginine-*p*-nitroaniline hydrochloride was added. After incubation for another 15 min at 30 °C, the reaction was stopped by adding 200  $\mu$ L of 10% acetic acid. The changes in absorbance at 410 nm were recorded at 30 °C against a blank solution containing 1.5 mL of the substrate solution in the same buffer with a Shimadzu UV mini-1240 spectrophotometer. One unit of inhibitor activity produced a 0.1 unit decrease in absorption of the solution in the trypsin activity assay. The inhibition constants ( $K_i$ s) for trypsin were measured using a Dixon plot ( $1/V_0$  against inhibitor), with two different substrate concentrations, 0.01 and 0.005  $\text{mol L}^{-1}$  for *N*- $\alpha$ -benzoyl-L-arginine ethyl ester hydrochloride.

### 2.8. Bioassay of Inhibition of Spore Germination and Hyphal Growth by Recombinant FtTI

Spore suspensions of *A. solani* were shaken vigorously for 2 min. A 0.1 mL aliquot of the suspension was dispensed into a microtube containing potato dextrose broth (Difco; 0.4 mL, 0.5%), and the recombinant *FtTI* protein was added [31]. After incubating *A. solani* spores for 6 h at 28 °C, germinated spores were counted using a hemocytometer and light microscope. Conidial suspensions of *A. solani* in potato dextrose broth were incubated in microtubes until the hyphae had an average length of 25  $\mu$ m. A 0.1 mL sample of the recombinant *FtTI* protein was then added to the conidial suspension. Various concentrations of the recombinant *FtTI* protein were used. The mixture was incubated at 30 °C until the control germlings attained an average length of approximately 300  $\mu$ m. The lengths of 50 individual hyphae were determined using a Nikon UFX-DX light microscope (Nikon, Tokyo, Japan). Hyphal lengths and conidial germination were determined, for each replicate, from at least ten randomly chosen germ tubes and 50 conidia, respectively.

### 2.9. Experimental Design and Statistical Analysis

All data are expressed as means  $\pm$  standard deviations (SDs) of three replications, and an Analysis of Variance (ANOVA) (SAS Inst. Inc., Cary, NC, USA) was carried out for the statistical analysis. The values were considered significantly or highly significantly different at  $p < 0.05$  and 0.01, respectively [32].

## 3. Results and Discussion

### 3.1. Cloning and Characterization of FtTI

PCR was used to amplify the conserved 147 bp fragment of *FtTI* that encoded 49 amino acids. A nucleic acid sequence alignment analysis showed no homology with the protease inhibitor genes of other higher flora and fauna, but this fragment showed a 42.8% homology with the *Xenopus (Silurana) tropicalis* (NM\_001114247.1) interleukin gene. The 49 amino acid sequence alignment analyses showed there is a 47–59% homology with the protease inhibitor-like proteins of other higher plants. The fragment was thought to be a new protease inhibitor. Genome walking was used to propagate the full-length DNA of *FtTI*. The gDNA sequence of the full-length *FtTI* was 644 bp.

A DNASTar software analysis showed an open reading frame between nt 207 and 472, encoding 87 amino acids. The 5' untranslated region was 207 bp in length, and the upstream sequence had two control elements and was GC rich. There was a conserved TATATT box upstream of the promoter at nt –25 to –35, and the start codon (ATG) was located at nt 209–211; the initial codon region sequence ATAATGT is a typical conserved region of the plant gene, with –3 bp being A/T, and +4 being T. The stop codon (TGA) was located at nt 469–471; the stop codon to the poly (A) tail for the noncoding region, in total 176 bp, was AT rich, including a typical AATAAA hex nucleotide polyadenylation signal sequence (Figure 1). There are no introns in the *FtTI* full-length sequence. Therefore, the coding sequence of the *FtTI* gDNA can be directly expressed in prokaryotic cells. A BLAST algorithm-based sequence homology analysis in GenBank showed that the gene's sequence was completely different from that of the plant protease inhibitor gene, and was a new gene in dicotyledonous plants. Where the inhibitor background is not understood, and no homologous sequence can be used for reference, primer design is difficult. In this study, the biggest difficulty in primer design was that the amino acids in the conserved region of the inhibitor protein sequence were mostly encoded by a highly degenerate codon, which is very unfavorable to the specificity of PCR amplification. Using the primary structure of the FiTI and the conserved amino acid sequences of protease inhibitors from common buckwheat and other plant species, WPELVG and CDRVW, with high homology levels, were found at the N- and C-termini. A partially degenerate codon was applied to clone its conserved region's sequence, and then genome walking was used to clone the full length of the FiTI gene for the first time.

```

ATATTTAGCACGAGGGCTGCTCGATGGCGATGGTACGTACGTTATGAGTTCAATAAGTTGAGCAATGACAGTGGTCAC
ATAATTAAC89..92TCAATCATCCACCTACACTACTTATTCTTATTTCCGTCCACATAATTTAATTTGTCTATCTCCTTCCAA
ATATCCCCATAGACATATATTACGTGGCATGTTGTCAACTAGACATATATAAT172..175GTTAATTTACGCTAAAGTTAAGTGT
M L I Y A K V K C
TTAATTACGGGTGTACGTACATACGTAGGTAACAGAGTTGGCCCGAGCTTGTGGAACCAAAGGGAAGACAGCTGCA
L I T G V R T Y V G K Q S W P E L V G T K G K T A A
GCCACCATAGATAAGGAGAATGCGCACGTACCGCGTCTCTGTGTCCTTTAACCCTCTAGCCACCTGCCGCACT
A T I D K E N A H V T A V L C P P L T T L A T C R T
TTCGACTTTCGTTGTGACCGGGTGCCTGTTTTAATTAATAGAATCGGCGGAGTTGTTACTAAGACCCCAACCGTCGGT
F D F R C D R V R V L I N R I G G V V T K T P T V G
TGA579..584ACTTGCAAAATCTCATGCAAGGCTTCATTTCTGTAATAGTACGTCATTTGAATAAGGGACGTTGCATTACAGTTA
Z
ATGTAACGTTGTAACATATGTAATTTACCACTGAATAAATTGCCTATTATTGTTGTAATAAAAAAAAAAACCTATAGTGAA
ATCACTAGTGGAGGATCCGC

```

**Figure 1.** Nucleotide sequences of *FtTI*. The open reading frame, from bases 208 to 471 predicts an 87 amino acid sequence before a stop signal (Z) is encountered. The promoter sequences, CAAT and TATA, in the 5'-untranslated region are from 89 to 92 and from 172 to 175, respectively. The poly (A) signal, AATAAA, in the 3'-untranslated region is from 579 to 584.

### 3.2. Expression and Purification of *FtTI* and *FtTI* Mutants

The major objective of this study was to determine whether the *FtTI* P1 loop is indeed the reactive site responsible for inhibiting trypsin and, in particular, whether Asp<sup>67</sup> and Arg<sup>68</sup> are involved in this inhibition. Three *FtTI* mutants of conserved active site amino acids and *FtTI* were independently produced in *E. coli* strain BL21 (DE3), an expression host designed for enhanced yields of active soluble recombinant proteins. The three mutants and recombinant *FtTI* were expressed in a pET-32a (+) vector, and the recombinant products, fused with His tags, were isolated, purified, and their inhibitory activity

levels measured. An SDS-PAGE analysis of the expressed product showed similar molecular weights for *FtTI* before and after the mutations, 9.5 kDa (Figure 2). Using *E. coli* BL21 (DE3) cells for expression, the yields of purified proteins recovered exclusively from the intracellular soluble fraction were 256 mg (D67V), 264 mg (R68L), 248 mg (R68L/D67V), and 287 mg (recombinant *FtTI*) per 1 L of culture. These expression levels are very similar to those reported for other recombinant plant protease inhibitors, such as mustard, mung bean and winged bean TIs, with yields of approximately 180–200 mg per 1 L of culture [4,5,26]. *E. coli* BL21 (DE3) cells were induced for 5 h with isopropyl  $\beta$ -D-thiogalactoside.

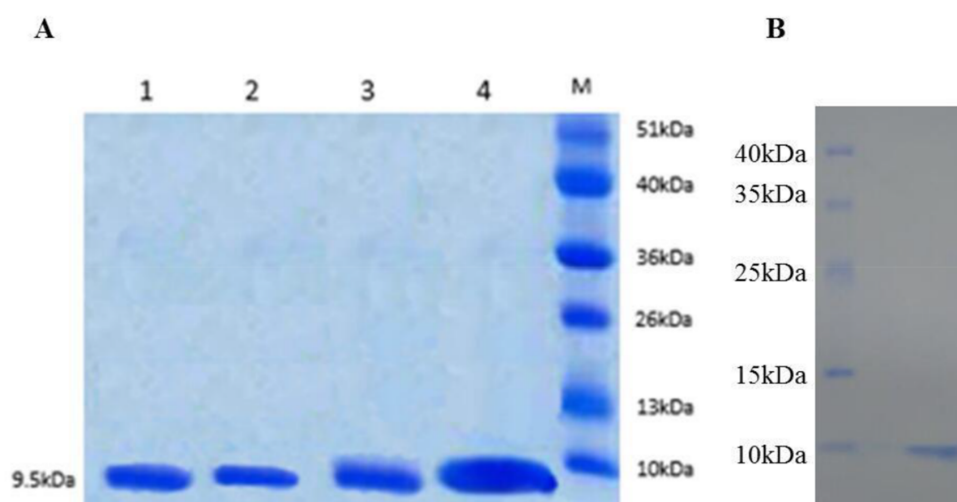


**Figure 2.** SDS-PAGE (A) and Western blot analysis (B) of recombinant *FtTI* and its mutants. (A) Lanes 1, 2, 3, 4, and M: recombinant *FtTI* mutants R65L, D67V, and R65L/D67V, recombinant *FtTI*, and molecular mass standards, respectively; (B) Western blot analysis of the purified recombinant protein.

### 3.3. Analyses of the Characteristics of Recombinant *FtTI* and Its Mutants

It has been reported that Asp<sup>67</sup> and Arg<sup>68</sup> are P1 residues of the potato protease inhibitor I family's active site [10]. Data obtained from a multiple alignment study of *FtTI* with a number of other similar TIs showed that the Arg or Asp residue of *FtTI* remained conserved among the proteins [24]. As shown in Table 1, we selected Asp<sup>67</sup> and Arg<sup>68</sup> for mutation to address two questions: (i) whether the positively charged (Arg<sup>68</sup>) or negatively charged (Asp<sup>67</sup>) N-terminal residue plays a role in stabilizing the inhibitory active site; and (ii) whether the simultaneous mutation of these two amino acids will lead to a more severe decline in inhibitory activity. *FtTI* was mutated by site-directed mutagenesis technology, and three mutant strains, D67V, R68L, and R68L/D67V, were obtained. The recombinant and mutated *FtTI* peptides had no inhibitory activity against chymotrypsin. The inhibition kinetics of the mutants D67V, R68L, and R68L/D67V, as well as the recombinant *FtTI* peptide for bovine trypsin and chymotrypsin, were assessed by determining the equilibrium dissociation constant  $K_i$  values using the Dixon plot. The  $K_i$  values for bovine trypsin were, respectively,  $3.3 \times 10^{-8}$  mo L<sup>-1</sup>,  $1.9 \times 10^{-8}$  mo L<sup>-1</sup>,  $1.8 \times 10^{-8}$  mo L<sup>-1</sup>, and  $1.62 \times 10^{-9}$  mo L<sup>-1</sup> (using *N*-benzoyl-DL-arginine-*p*-nitroaniline hydrochloride as substrate; Figure 3). The variants D67V and R68L were found to have only 1–2% of the *FtTI* activity. This indicated that the inhibitor contains at least one reactive site where the P1 residues Asp<sup>67</sup> and Arg<sup>68</sup> are capable of binding one molecule of trypsin. This discovery is consistent with previous results [33]. The electron densities of the P1 residues of the reactive site matched perfectly with those of residues Asp<sup>67</sup> and Arg<sup>68</sup>, as reported previously [4,10,32,33]. We suggest that the fully functional recombinant *FtTI* lost its trypsin inhibitory activity when its Asp<sup>67</sup> or Arg<sup>68</sup> residues were mutated. Of the P1-amino acid mutants studied, two amino acid residues in the site had essentially no trypsin inhibitory activities [10]. These had mutations at either Asp<sup>67</sup> or Arg<sup>68</sup>, the negatively and positively charged residues, respectively, near

the middle of the active site. The present work on *FtTI* further indicates that, even for the TI of this family, the inhibitory mechanism can also vary. Because of the presence of P1, neither residue Asp<sup>67</sup> nor Arg<sup>68</sup> at the reactive site of the D67V, R68L, and R68L/D67V mutants is favorable for trypsin binding; therefore, the mutants show quite weak inhibitory activity levels. The inhibitory activity of a protease inhibitor results from its ability to form a stable complex with the target protease, thereby blocking, altering, or preventing the substrate from entering the enzyme's active site [8,34].

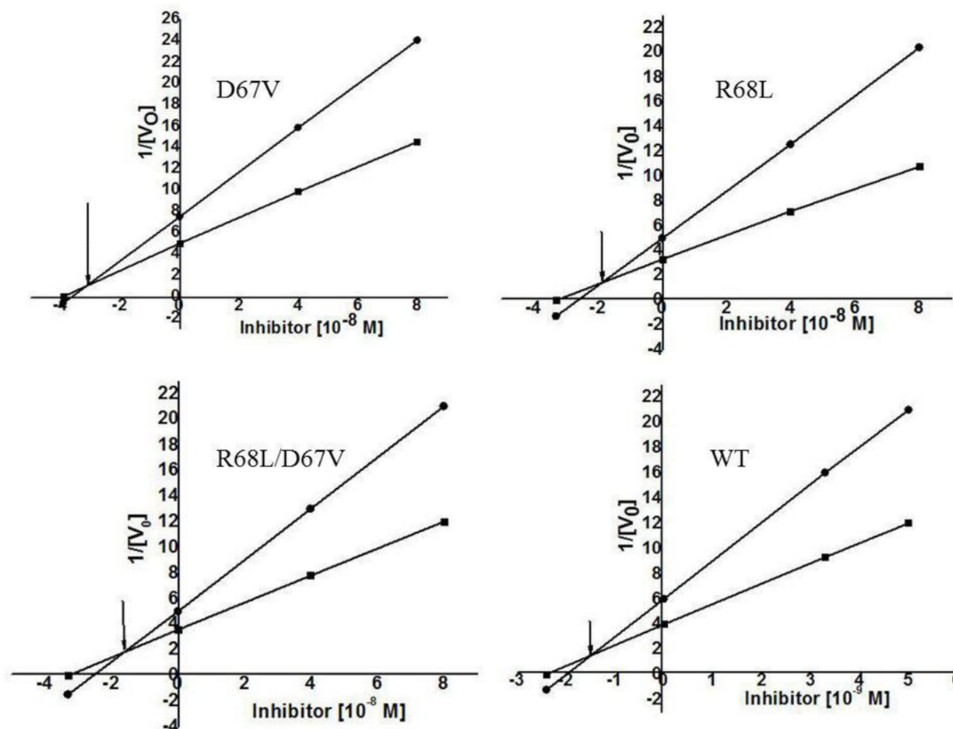


**Figure 3.** Kinetic analysis of the trypsin inhibitory activity of *FtTI*. Dixon plot for the determination of the dissociation constant ( $K_i$ ) values of *FtTI* at two different concentrations of *N*- $\alpha$ -benzoyl-L-arginine ethyl ester hydrochloride. Final substrate concentrations were 0.01 M (■) and 0.005 M (▲). The reciprocals of velocity were plotted against different concentrations of *FtTI*.

In summary, three *FtTI* mutants obtained by site-directed mutagenesis were used to investigate the structure–function relationship of the trypsin inhibitory activity. The study generated a series of results that appear to deviate from previous results related to how the P1 inhibitory active site of the potato protease inhibitor I family works and is stabilized. Most notably, our result indicated that the two amino acid residues in the *FtTI* P1 active site residues, Asp<sup>67</sup> and Arg<sup>68</sup>, are critical for the inhibitory function, which conflicts with the long-held belief that only a positively charged amino acid is required. Our discovery thus suggests that trypsin inhibitory mechanisms are more complicated than previously thought, and should be the topic of renewed interest in further research on the potato protease inhibitor I family, especially its less well-known members.

### 3.4. In-Vitro Antifungal Activity of Recombinant *FtTI*

To determine whether the recombinant *FtTI* protein has a direct antifungal effect, it was purified from *FtTI*-expressing *E. coli*. The antifungal activity of the purified recombinant *FtTI* protein at various concentrations was tested against *A. solani* using a microtiter broth dilution assay. The purified recombinant *FtTI* protein completely inhibited *A. solani* mycelial growth at 50  $\mu\text{g mL}^{-1}$  (Figure 4A). Fungal conidial germination was inhibited by recombinant thioredoxin-*FtTI* protein, but not by thioredoxin alone (Figure 4B). Treatment with 100  $\mu\text{g mL}^{-1}$  *FtTI* completely inhibited conidial



germination (Figure 4B). At  $1 \mu\text{g mL}^{-1}$ , *FtTI* did not suppress *A. solani* spore germination. However, *A. solani* spore germination was strongly inhibited at 5 and  $10 \mu\text{g mL}^{-1}$  *FtTI*. The hyphal growth of *A. solani* was completely inhibited at 50 and  $100 \mu\text{g mL}^{-1}$  *FtTI*. These results indicate that the recombinant *FtTI* antifungal protein directly affects the mycelial growth and spore germination of fungal pathogens. Many plants respond to fungal attack by accumulating TI as a method of blocking fungal hyphal growth. TI production is one of the earliest cytological detectable responses to infection by fungal species. TIs also play vital roles in plant natural defenses against fungal infections. The function of *FtTI* in plant defense mechanisms has been extensively investigated, either in vivo using *FtTI* to fight plant-pathogenic microorganisms [24], or in vitro using native or recombinant *FtTI* to control lepidopteran pests [21,25]. In comparison with the recombinant *FtTI*, the inhibition of mycelial growth and spore germination by mutants D67V, R68L, and R68L/D67V decreased significantly, leading to a pronounced increase in the lengths of the mycelia and the numbers of conidia of *A. solani* (Figure 4). As shown by the arrows in Figure 5, compared with the control, the hyphal tips of the treatment group were deformed, the mycelial volumes were decreased, and no conidia were generated.

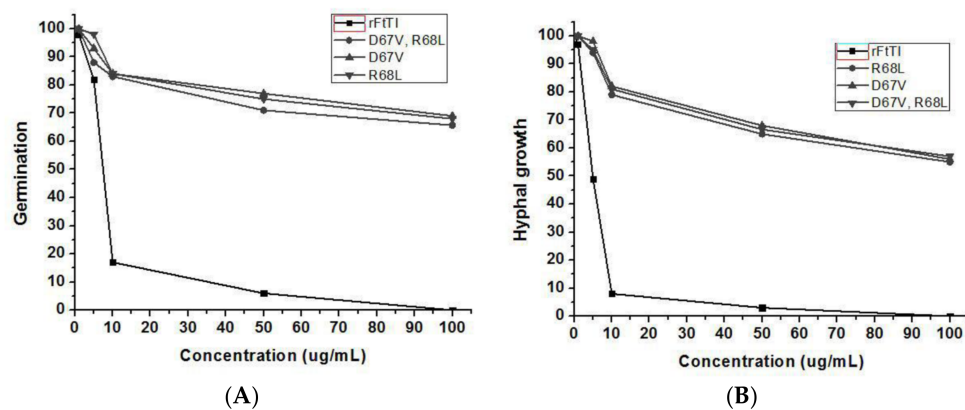


**Figure 4.** Inhibitory effects of the recombinant *FtTI* protein at various concentrations on the hyphal growth (A) and conidial germination (B) of *A. solani*. The results are expressed as relative values compared to those of untreated controls (set to 100%).

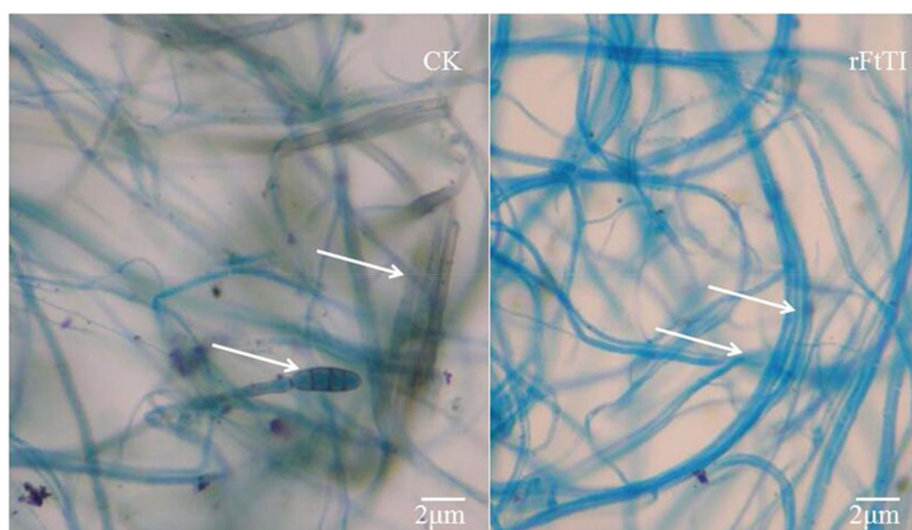


**Figure 5.** In vitro hyphal morphology studies. Left, hyphal morphology of *Alternaria solani* in a control well. Right, hyphal morphology of *A. solani* in a protein-treated well. Deformations of the hyphal tips (arrows) and decreases in mycelial volume compared to the control.

Thus, we identified a novel anti-phytopathogen gene, *FtTI*, which was isolated from tartary buckwheat leaves infected with *A. solani*. The molecular inhibitory mechanism of *FtTI* against plant-pathogenic fungal spore germination and mycelial growth remains unknown. On the one hand, phytopathogenic fungi need to hydrolyze proteases during the process of infection and spread to obtain nutrients. On the other, weaker protease-inhibitor interactions might result in lower concentrations of the protease-inhibitor complexes that are perceived by *FtTI*, thus repressing plant-pathogenic fungal protease secretion upon spore germination and mycelial growth. The elucidation of the three-dimensional structures of *FtTI* in complex with proteases secreted by phytopathogenic fungi will help determine whether slight changes in the vital amino acids of the *FtTI* active site form the basis of mutual recognition by the protease-inhibitor complex. The blockage of phytopathogenic fungal signaling pathways and molecular mechanisms by plant protease inhibitors warrants further study.

#### 4. Conclusions

Molecular cloning, expression, and site-mutation studies enabled the characterization of a TI from tartary buckwheat. Purified recombinant *FtTI* exhibited strong in vitro antifungal activities against *A. solani* phytopathogenic fungi. A multiple sequence alignment with related inhibitors and site-directed mutagenesis indicated that the Asp<sup>67</sup> and Arg<sup>68</sup> residues are essential for *FtTI*'s inhibitory activity, as further substantiated by the mutational study of this TI.

**Supplementary Materials:** The following are available online at <http://www.mdpi.com/2073-4395/8/4/46/s1>.

**Acknowledgments:** This research was financially supported by the Regional Funds of the National Natural Science Foundation of China (No. 31660531) and Guizhou University to Introduce Talent Research Projects (No. 2016040). We are very grateful Ming-jian Ren (Guizhou Sub-center of the National Wheat Improvement Center) for fruitful discussions on this work. We also acknowledge Prof. Guoshu Gong (Sichuan Agricultural University) and Lei Lei (Institute of Plant Protection of the Chinese Agricultural Academy of Sciences, Beijing, China) for anti-fungal tests.

**Author Contributions:** J.-j.R. and J.-p.C. designed research; J.-j.R., S.-j.T., H.C. and R.-h.X. performed research; H.C. contributed new reagents/analytic tools; H.C. and J.Y. analyzed data; and J.-j.R. and J.-p.C. wrote the paper.

**Conflicts of Interest:** The authors declare no conflict of interest.

#### References

- Gaspar, Y.M.; McKenna, J.A.; McGinness, B.S.; Hinch, J.; Poon, S.; Connelly, A.A.; Anderson, M.A.; Heath, R.L. Field resistance to *Fusarium oxysporum* and *Verticillium dahliae* in transgenic cotton expressing the plant defensin NaD1. *J. Exp. Bot.* **2014**, *65*, 1541–1550. [[CrossRef](#)] [[PubMed](#)]
- Tomazoni, E.Z.; Pauletti, G.F.; da Silva Ribeiro, R.T.; Moura, S.; Schwambach, J. In vitro and in vivo activity of essential oils extracted from *Eucalyptus staigeriana*, *Eucalyptus globulus* and *Cinnamomum camphora* against *Alternaria solani* Sorauer causing early blight in tomato. *Sci. Hortic.* **2017**, *223*, 72–77. [[CrossRef](#)]
- Bathige, S.D.N.K.; Umasuthan, N.; Godahewa, G.I.; Jayasinghe, J.D.H.E.; Whang, I.; Noh, J.K.; Lee, J. A homolog of kunitz-type serine protease inhibitor from rock bream, *Oplegnathus fasciatus*: Molecular insights and transcriptional modulation in response to microbial and pamp stimulation, and tissue injury. *Fish Shellfish Immunol.* **2015**, *46*, 285–291. [[CrossRef](#)] [[PubMed](#)]
- Qi, R.F.; Liu, Z.X.; Xu, S.Q.; Zhang, L.; Shao, X.X.; Chi, C.W. Small peptides derived from the Lys active fragment of the mung bean trypsin inhibitor are fully active against trypsin. *FEBS J.* **2010**, *277*, 224–232. [[CrossRef](#)] [[PubMed](#)]
- Volpicella, M.; Leoni, C.; Arnesano, F.; Gallerani, R.; Ceci, L.R. Analysis by phage display selection and site-directed retromutagenesis of the Mustard Trypsin Inhibitor 2 reactive site. *J. Plant Physiol.* **2010**, *167*, 1507–1511. [[CrossRef](#)] [[PubMed](#)]
- Ekchaweng, K.; Khunjan, U.; Churngchow, N. Molecular cloning and characterization of three novel subtilisin-like serine protease genes from *Hevea brasiliensis*. *Physiol. Mol. Plant Pathol.* **2017**, *97*, 79–95. [[CrossRef](#)]

7. Liu, D.; Li, Y.; Man, L.; Wu, Q.; Liu, S.; Liu, Y. Molecular cloning and characterization of PtrZPT2-1, a ZPT2 family gene encoding a Cys2/His2-type zinc finger protein from trifoliolate orange (*Poncirus trifoliata*, (L.) Raf.) that enhances plant tolerance to multiple abiotic stresses. *Plant Sci. Int. J. Exp. Plant Biol.* **2017**, *263*, 66–78. [[CrossRef](#)] [[PubMed](#)]
8. Shamsi, T.N.; Parveen, R.; Naz, H.; Haque, M.A.; Fatima, S. Biophysical insight into structure-function relation of *Allium sativum* Protease Inhibitor by thermal, chemical and pH-induced modulation using comprehensive spectroscopic analysis. *Int. J. Biol. Macromol.* **2017**, *103*, 415–423. [[CrossRef](#)] [[PubMed](#)]
9. Júnior, J.E.M.; Valadares, N.F.; Pereira, H.D.; Dyszy, F.H.; da Costa Filho, A.J.; Uchôa, A.F.; de Oliveira, A.S.; da Silveira Carvalho, C.P.; Grangeiro, T.B. Expression in *Escherichia coli* of cysteine protease inhibitors from cowpea (*Vigna unguiculata*): The crystal structure of a single-domain cystatin gives insights on its thermal and pH stability. *Int. J. Biol. Macromol.* **2017**, *102*, 29–41. [[CrossRef](#)] [[PubMed](#)]
10. Yao, P.L.; Hwang, M.J.; Chen, Y.M.; Yeh, K.W. Site-directed mutagenesis evidence for a negatively charged trypsin inhibitory loop in sweet potato sporamin. *FEBS Lett.* **2001**, *496*, 134–138. [[CrossRef](#)]
11. Yu, Q.; Ryan, E.M.; Allen, T.M.; Birren, B.W.; Henn, M.R.; Lennon, N.J. PriSM: A primer selection and matching tool for amplification and sequencing of viral genomes. *Bioinformatics* **2011**, *27*, 266–267. [[CrossRef](#)] [[PubMed](#)]
12. Boyce, R.; Chilana, P.; Rose, T.M. iCODEHOP: A new interactive program for designing CONsensus-DEgenerate Hybrid Oligonucleotide Primers from multiply aligned protein sequences. *Nucleic Acids Res.* **2009**, *37*, 222–228. [[CrossRef](#)] [[PubMed](#)]
13. René, O.; Alix, J.H. Late steps of ribosome assembly in *E. coli* are sensitive to a severe heat stress but are assisted by the HSP70 chaperone machine. *Nucleic Acids Res.* **2011**, *39*, 1855–1867. [[CrossRef](#)] [[PubMed](#)]
14. Brand, G.D.; Pires, D.A.T.; Furtado, J.R.; Cooper, A.; Freitas, S.M.; Bloch, C., Jr. Oligomerization affects the kinetics and thermodynamics of the interaction of a Bowman-Birk inhibitor with proteases. *Arch. Biochem. Biophys.* **2017**, *618*, 9–14. [[CrossRef](#)] [[PubMed](#)]
15. Gorrón, E.; Rodríguez, F.; Bernal, D.; Rodríguez-Rojas, L.M.; Bernal, A.; Restrepo, S.; Tohme, J. A new method for designing degenerate primers and its use in the identification of sequences in *Brachiaria* showing similarity to apomixis-associated genes. *Bioinformatics* **2010**, *26*, 2053–2054. [[CrossRef](#)] [[PubMed](#)]
16. Evans, B.A.; Hamouda, A.; Towner, K.J.; Amyes, S.G. Novel genetic context of multiple bla OXA-58 genes in *Acinetobacter* genospecies 3. *J. Antimicrob. Chemother.* **2010**, *65*, 1586–1588. [[CrossRef](#)] [[PubMed](#)]
17. Zhu, F. Chemical composition and health effects of Tartary buckwheat. *Food Chem.* **2016**, *203*, 231–245. [[CrossRef](#)] [[PubMed](#)]
18. Bai, C.Z.; Feng, M.L.; Hao, X.L.; Zhao, Z.J.; Li, Y.Y.; Wang, Z.H. Anti-tumoral effects of a trypsin inhibitor derived from buckwheat in vitro and in vivo. *Mol. Med. Rep.* **2015**, *12*, 1777–1782. [[CrossRef](#)] [[PubMed](#)]
19. Khadeeva, N.V.; Kochieva, E.Z.; Tcherednitchenko, M.Y.; Yakovleva, E.Y.; Sydoruk, K.V.; Bogush, V.G.; Dunaevsky, Y.E.; Belozersky, M.A. Use of buckwheat seed protease inhibitor gene for improvement of tobacco and potato plant resistance to biotic stress. *Biochemistry (Mosc.)* **2009**, *74*, 260–267. [[CrossRef](#)] [[PubMed](#)]
20. Park, S.S.; Ohba, H. Suppressive activity of protease inhibitors from buckwheat seeds against human T-acute lymphoblastic leukemia cell lines. *Appl. Biochem. Biotechnol.* **2004**, *117*, 65–74. [[CrossRef](#)]
21. Wang, Z.; Li, S.; Ren, R.; Li, J.; Cui, X. Recombinant buckwheat trypsin inhibitor induces mitophagy by directly targeting mitochondria and causes mitochondrial dysfunction in Hep G2 cells. *J. Agric. Food Chem.* **2015**, *63*, 7795–7804. [[CrossRef](#)] [[PubMed](#)]
22. Ashouri, S.; Abad, R.F.P.; Zihnioglu, F.; Kocadag, E. Extraction and purification of protease inhibitor (s) from seeds of *Helianthus annuus* with effects on *Leptinotarsa decemlineata* digestive cysteine protease. *Biocatal. Agric. Biotechnol.* **2017**, *9*, 113–119. [[CrossRef](#)]
23. Qian, C.; Liang, D.; Liu, Y.; Wang, P.; Kausar, S.; Wei, G.; Zhu, B.; Wang, L.; Liu, C. Identification of a small pacifastin protease inhibitor from *Nasonia vitripennis* venom that inhibits humoral immunity of host (*Musca domestica*). *Toxicon* **2017**, *131*, 54–62. [[CrossRef](#)] [[PubMed](#)]
24. Ruan, J.J.; Chen, H.; Shao, J.R.; Wu, Q.; Han, X.Y. An antifungal peptide from *Fagopyrum tataricum* seeds. *Peptides* **2011**, *32*, 1151–1158. [[CrossRef](#)] [[PubMed](#)]
25. Ruan, J.; Yan, J.; Hou, S.; Chen, H.; Wu, Q.; Han, X. Expression and purification of the trypsin inhibitor from tartary buckwheat in *Pichia pastoris* and its novel toxic effect on *Mamestra brassicae* larvae. *Mol. Biol. Rep.* **2015**, *42*, 209–216. [[CrossRef](#)] [[PubMed](#)]

26. Bhattacharjee, N.; Banerjee, S.; Dutta, S.K. Cloning, expression and mutational studies of a trypsin inhibitor that retains activity even after cyanogen bromide digestion. *Protein Expr. Purif.* **2014**, *96*, 26–31. [[CrossRef](#)] [[PubMed](#)]
27. Lee, H.; Ren, J.; Nocadello, S.; Rice, A.J.; Ojeda, I.; Light, S.; Minasov, G.; Vargas, J.; Nagarathnam, D.; Anderson, W.F.; et al. Identification of novel small molecule inhibitors against NS2B/NS3 serine protease from Zika virus. *Antivir. Res.* **2017**, *139*, 49–58. [[CrossRef](#)] [[PubMed](#)]
28. Wang, C.; Zhang, H.; Li, M.; Hu, X.Q.; Li, Y. Functional analysis of truncated and site-directed mutagenesis dextranases to produce different type dextrans. *Enzyme Microb. Technol.* **2017**, *102*, 26–34. [[CrossRef](#)] [[PubMed](#)]
29. Laemmli, U.K. Cleavage of structural proteins during the assembly of the head of bacteriophage T4. *Nature* **1970**, *227*, 680–685. [[CrossRef](#)] [[PubMed](#)]
30. Matsudaira, P. Sequence from picomole quantities of proteins electroblotted onto polyvinylidene difluoride membranes. *J. Biol. Chem.* **1987**, *262*, 10035–10038. [[PubMed](#)]
31. Lee, S.C.; Hwang, I.S.; Choi, H.W.; Hwang, B.K. Involvement of the pepper antimicrobial protein CaAMP1 gene in broad spectrum disease resistance. *Plant Physiol.* **2008**, *148*, 1004–1020. [[CrossRef](#)] [[PubMed](#)]
32. Gibaud, A.; Vogt, N.; Brison, O.; Debatisse, M.; Malfoy, B. Characterization at nucleotide resolution of the homogeneously staining region sites of insertion in two cancer cell lines. *Nucleic Acids Res.* **2013**, *41*, 8210–8219. [[CrossRef](#)] [[PubMed](#)]
33. Ambadapadi, S.; Zheng, D.; Munaswamy-Ramanujam, G.; Lucas, A. Serine protease inhibitor (serpin) reactive center loop peptides as therapy for inflammatory vasculitis, hemorrhage and acute viral sepsis. *Atherosclerosis* **2015**, *241*, e209. [[CrossRef](#)]
34. Bao, R.; Zhou, C.Z.; Jiang, C.; Lin, S.X.; Chi, C.W.; Chen, Y. The ternary structure of the double-headed arrowhead protease inhibitor API-A complexed with two trypsins reveals a novel reactive site conformation. *J. Biol. Chem.* **2009**, *284*, 26676–26684. [[CrossRef](#)] [[PubMed](#)]



© 2018 by the authors. Licensee MDPI, Basel, Switzerland. This article is an open access article distributed under the terms and conditions of the Creative Commons Attribution (CC BY) license (<http://creativecommons.org/licenses/by/4.0/>).